Radon surveys and real-time monitoring at Stromboli volcano: influence of soil temperature, atmospheric pressure and tidal forces on 222Rn degassing.

DOI:10.1016/j.jvolgeores.2009.04.019

(Article begins on next page)

doi:10.1016/j.jvolgeores.2009.04.019
http://www.sciencedirect.com/science/article/pii/S0377027309002078

Cigolini C.[1], Poggi P.[2], Ripepe M.[3], Laiolo M. [1], Ciamberlini C. [2], Delle Donne D. [3], Ulivieri G. [3], Coppola D. [1], Lacanna G. [3], Marchetti E. [3], Piscopo D. [1], Genco R. [3]

1. *DSMP Università di Torino*
2. *INOA, Florence*
3. *DST Università di Firenze*

Radon surveys and real-time monitoring at Stromboli volcano: influence of soil temperature, atmospheric pressure and tidal forces on ^{222}Rn degassing

We used a network of stations to perform systematic radon surveys at Stromboli volcano. The time series of periodic measurements show that monthly average ^{222}Rn emissions reflect changes in volcanic activity and exhibit increasing trends prior and during the last major eruptive cycles. Maps of radon emissions indicate that diffuse degassing is operative at Stromboli volcano. Concentrated degassing essentially occurs in the summit area and within a sector proximal to the two major NE trending faults. These sites were chosen for deploying the two real-time stations that are currently operating at Stromboli. In these devices, the ^{222}Rn electronic dosimeters are interfaced with an electronic board connected to a radiomodem for wireless data transfer to a receiving station at the volcano observatory. Radon activity, soil temperature and atmospheric pressure data are sampled and instantaneously transferred via web so that they can be checked in remote. Collected time series reveal an overall inverse correlation between radon emissions and seasonal temperature variations. Signal processing analysis show that radon emissions in sectors of diffuse degassing are modulated by tidal forces as well. Radon activities recorded at the summit station, located along the fracture zone where the gas flux is concentrated, are positively correlated with changes in atmospheric pressure and confirm the occurrence of the "atmospheric stack effect". It is not excluded that this process may play an active role, together with self-sealing of hydrothermal fractures, in modulating Stromboli explosivity. We finally emphasize that real-time radon monitoring is an innovative technique that may be systematically applied in volcano surveillance.

Introduction

Stromboli volcano is a unique natural laboratory to investigate complex magmatic processes including gaseous transfer to the surface. When an undegassed magma batch is approaching the subvolcanic environment, the gas phase starts to exsolve generating a "two-phase system". During magma ascent, gas expansion may produce variable explosive activities together with significant anomalies that may be detected in soils and/or within the volcanic plume as a result of shallow magma degassing (e.g., Allard et al., 1994; Chiodini et al., 1996, Heiligmann et al., 1997; Ripepe et al., 2005, among others). Following the last two major eruptive cycles (2002-03 and 2007) a multidisciplinary effort was undertaken in order to integrate geophysical and geochemical data.

Among these, radon monitoring has been acquiring a basic role in recording variations in volcanic activity as well as in detecting complex geodynamic processes associated to active tectonics. In nature, radon is mainly represented by the isotope ^{222}Rn (with a half life of 3.82 days): it is an alpha emitting radioactive gas produced from the decay of ^{226}Ra, in turn derived from uranium bearing materials. Marked radon anomalies may precede earthquakes (e.g., Fleischer and Mogro-Campero, 1985; Igarashi et al., 1995; Planicić et al., 2004) and volcanic eruptions (Chirkov, 1975; Connors et al., 1996; Cigolini et al., 2005; Alparone et al., 2005). In contrast to findings at Mount Etna, where an halo of magmatic CO_2 has been postulated to extend over much of the cone, Williams-Jones et al. (2000) have shown that Rn, CO_2 and δ^{13}C values are higher on the lower flanks of Arenal, Poás and Galeras volcanoes, except near the fumaroles surrounding the active craters. In addition, Varley and Armienta (2001) pointed out that diffuse degassing seems to absent at Popocatepetl volcano. However, these features may derive from self-sealing processes that affect the fracture networks of the hydrothermal shells surrounding magmatic systems and may not be permanent in space and time (cf., Cigolini et al., 2001).

In recent papers, some of us stressed the importance of deploying radon networks to detect major radon anomalies on active volcanoes by means of periodic measurements, thus identifying the sites of more efficient response to seismic transients and/or volcanic degassing (Cigolini et al., 2001; 2007). These sites are the ones that could be successfully used in locating stations for continuous radon monitoring. Automatic alpha particles detectors play a key-role in volcano surveillance contributing to decode the interplay among seismic signals and others geochemical parameters. Indeed, these may reveal critical variations before and during the onset of volcanic eruptions. Thus, systematic time series analysis and signal processing give us the opportunity for better understanding the dynamic behaviour of volcanoes.

In this paper we summarize some of the data collected during our periodic surveys and present the recent results of “real time” radon monitoring at Stromboli volcano. We first introduce the methods for ^{222}Rn measurements, and then discuss the time-series for radon emissions, soil temperatures, and atmospheric pressure.

Stromboli volcano and its last major eruptions

Stromboli is the north-eastern island of the Aeolian arc (Fig. 1). It is located on the Stromboli-Panarea alignment: a NE-SE strike-slip fault connected to the Tindari-Letojanni fault that propagates though Eastern Sicily and underlays Mount Etna. The Aeolian islands grew within the last 1.3 m.y. (Gillot and Keller, 1993), and the outcropping lavas and tephra are subduction-related calcalkaline, HK-calcalkaline, shoshonitic and potassic suites (Barberi et al., 1974; Beccaluva et al., 1985).

Stromboli volcano rises 924 m above sea level but most of the edifice, of unknown age, is extending ~2 km below sea-level. The exposed sector of the cone was formed during the last 100 kyr. Volcanic activity is essentially strombolian, with mild and continuous eruptions of ash, lapilli, scoriae and bombs (Rosi et al., 2000) from the summit craters, located at an average altitude of about 700 m a.s.l.. The typical and persistent activity may be episodically replaced by lava effusions, major explosions and paroxysms (with ejections of ballistic projectiles of several tons that may threaten the whole island). The latters may be associated with the origin of tsunamis, essentially related to flank failure on Sciara del Fuoco (a horseshoe-shaped scarp opening north-westward; e.g., Tibaldi, 2001) that may include portions of its submerged part. However, the generation of tsunamis waves may affect sectors of the West-Central Mediterranean region and are regarded as major risk factors in terms of civil defense (Barberi et al., 1993; Tinti et al, 2006).

The Stromboli hydrothermal system is subdivided into an upper portion that includes those sectors surrounding the conduit and the crater area, and a lower portion placed at the base of the cone with the upwelling of thermal springs in the village of Stromboli (Finizola et al., 2002; Carapezza et al., 2004). Radon surveys by Cigolini et al. (2005) have shown that the areas of major degassing are located on NE flank, and coincide with the most active sectors of the hydrothermal system. These are the ones that respond more efficiently to the onset of regional seismic transients.

The first of the most recent major eruptive cycle started on December 28, 2002 with the effusion of a lava flow that was followed by a composite slump onto Sciara del Fuoco generating a tsunamis that damaged the northern part of Stromboli and affected the coast of northeastern Sicily. Lava effusion persisted until July 21, 2003 and was ongoing during the paroxysmal explosion of April 5, 2003 (Bonaccorso et al., 2003; Ripepe et al., 2005; Calvari et al., 2005). The geochemical anomalies that preceded these two eruptive events were discussed by Carapezza et al. (2004), whereas Ripepe et al. (2005) outlined the relationships among VLP signals, thermal anomalies and SO_2 plume degassing.

The typical mild Strombolian activity resumed by the end of July 2003 and persisted until February 27, 2007, when a new lava flow effused from the NE crater. Lava discharge has been continuous until April 2, 2007 (essentially from a lower vent located at 400 m a.s.l. that replaced the lava outflow from the summit crater few hours after the onset of the eruption). The most recent paroxysmal explosion occurred on March 15, 2007, from the summit craters with the ejection of bombs and projectiles that fell just 150 m above the houses of Stromboli village. This event was preceded by a drastic increase in volcanic seismicity and was followed by the vertical collapse (of about 150 m from its original altitude) of the summit craters' floor (in the night of March 24, 2007). Following a transitional phase (characterized by moderate seismic and infrasonic activity, and absence of explosions at the summit vents) the mild Strombolian activity was finally resumed by the end of June-beginning of July, 2007 and is currently on-going. A detailed description of the 2007 Stromboli eruption has been given by Barberi et al. (2008) and Neri and Lanzafame (2008). In addition, geochemical data on precursory signals are reported by Rizzo et al. (2008).

FIG. 1

Summary of previous radon surveys

We started our periodic radon surveys in May 2002. We deployed a network of 25 stations (Fig. 1) that have been subdivided into three groups: summit stations (around the crater area) lower stations (below 100 m a.s.l.) and other stations (intermediate in altitude between the cited groups). Measurements were first performed by track-etch detectors (LR115, finely calibrated according to Bonetti et al., 1991) exposed from two to five weeks. During our periodic surveys we also utilized E-PERM® electretes (Kotrappa et al., 1993) that were exposed from one to four days. In both cases, these detectors were collected manually giving integrated measurements of radon activity during their time of exposure. Both detectors were placed in subsurface pipe-like samplers (1.20 m long with a diameter of 12 cm, which were set to a depth of about 60 cm) isolated by a cap to minimise condensation.

Following the major eruptive cycle that started on December 28, 2002, we performed repeated and systematic surveys to be able to correlate radon emissions with changes in volcanic activity (Cigolini et al., 2005). The use of the above detectors (exposed contemporaneously for all the stations of the network) gave us the opportunity to better discriminate the effects of regional seismicity on radon degassing from those related to variations in volcanic activity (e.g., Cigolini et al., 2007). In addition, we identified those sectors of the volcano that better respond to changes in volcanic activity and/or seismic transients. The results of these systematic surveys were summarized in the cited papers, and some precursory signals were analyzed as well. In summary, major eruptive events were preceded by relative minima in radon emissions at stations located at the base of the cone, whereas three of the summit stations reached threshold values (~20,000 Bq/m^3 or higher) 12 to 14 days before the onset of major eruptions, and were nearly coeval with earth tides. Conversely, relative minima recorded at the base of the cone were related to fractures' *self-sealing* within the hydrothermal system, eventually coupled with the *"atmospheric stack-effect"* that substantially reduced the efficiency of hydrothermal convection. An overview of a whole set of geochemical data on this eruption have been reported by Federico et al. (2008). The typical mild Strombolian activity resumed by the end of July 2003, and persisted until February 27, 2007, when a new lava flow effused from the NE crater. During this span of time periodic surveys were preformed regularly (a summary of the data is reported in Fig. 2). It can be noticed, from the monthly histograms of average radon emissions, that there is an increasing trend both before the onset of the last two major eruptive cycles for all the stations of the network. Higher emissions persist throughout the duration of both the effusive cycles. Moreover, monthly average emissions indicate that

FIG. 2

Following the onset of the last effusive cycle, that started on February 27, 2007, lava discharge has been continuous until April 2, 2007 (essentially from a lower vent located at 400 m a.s.l.). The most recent paroxysmal explosion occurred on March 15, 2007, from the summit craters with the ejection of bombs and projectiles that fell just 150 m above the houses of Stromboli village. In Fig. 3 we report the maps for radon emissions recorded prior and during the onset and development of the last major eruptive cycles at the 25 stations of the network. Average radon activities for each stations have been plotted onto topographic DEM images to show the sectors of higher ^{222}Rn concentration. It may be noted that higher emissions are mainly confined to the summit area and the two major summit faults trending N40°E and N60°E (e.g., Finizola et al., 2002), where average radon activities are well above 15000 Bq/m^3. However, other sectors of the cone have moderately high radon emissions that may reach 5000-6000 Bq/m^3. In Table 1 we summarize the statistical results obtained for on over 2300 measurements collected during our surveys since May 2002, that show the average values for background, threshold and anomalies (calculated according to Hernandez, 2004; following the principles of Sinclair, 1974) for the stations of the network.. It may be observed that average background values for most stations, excluding those of the summit, are generally well above 1000 Bq/m^3. However, Cigolini et al. (2005; 2007) have shown that the areas of major degassing on the NE flank coincide with the geometry of the most active sectors of the hydrothermal system where some of the lower stations may reach average values of 15000 Bq/m^3 or higher. This indicates that radon emissions may fluctuate under variable dynamic conditions (that reflect changes in the volcanic activity and/or the onset of seismic transients) and support the idea that diffuse degassing is operative and efficient in the exposed sector of Stromboli volcano.

FIG. 3 **TABLE 1**

Real Time Methods

Real-time stations for continuous radon monitoring were constructed by integrating the electronic radon dosimeter DOSEman (produced by Sarad GmbH, Dresden, Germany) with an electronic board that transfer the output signal to a radio modem. This communicates through a directional antenna with a receiving station at the volcano observatory. Sampling time for radon measurements (and related gaseous progeny) and environmental parameters (local soil temperature and atmospheric pressure) is 15 minutes. Data are instantaneously elaborated and plotted as time series on a PC screen and are transferred via web so that they can be checked in remote.

Technical details for the electronic radon dosimeter are given in details by Streil et al. [2002] and Gründel e Postendörfer (2003). In DOSEman, the radon gas diffuses trough a leather membrane into a measurement chamber (cylindrical in shape and 12 cm^3 in volume). Here the charged radon particles (including its progeny) are collected onto a semiconductor detector and are measured by means of alpha spectrometry. Thus, the radon alpha decays are registered and processed by a multichannel analyser that subdivides the counts into Regions of Interest (named ROIs). Therefore the spectrum for the radon gas source is obtained (Fig. 4) and radon activity can be retrieved by using the peak areas of ^{222}Rn, ^{218}Po and ^{214}Po. Similarly, the activity of ^{220}Rn (thoron) can be measured. This isotope is regarded as a key-parameter to discriminate between local degassing (i.e. ^{220}Rn, essentially related to soil) and deep degassing (^{222}Rn and related progeny, also released from an endogenous source) (e.g., Giammanco et al., 2007). The statistical error at radon concentration of 1000 Bq/m^3 has been estimated to be ± 25% and exponentially decreases at higher emissions (Streil et al., 2002).

FIG. 4

A single station consists of the electronic radon dosimeter interfaced with the electronic board that are stored, together with the radio modem, in a polycarbonate case permeable to radon. The case has been positioned within a PVC box (open downward) confined into soil down to a depth of about 100 cm. This cavity occupied by “free soil air” and releases the gas flux into the atmosphere through a tube interconnected with a minor cylindrical “expansion reservoir” that attenuates the effects of atmospheric perturbations. Average radon measurements are perfectly compatible with those obtained by track-etch detectors exposed at the same sites for the same amount of time. In Fig. 5 we report the positioning of the PZZ station at the summit of Stromboli.

FIG. 5

Real-time radon monitoring

In this section we will present and analyze the data collected for over a year at the Liscione station (LSC), together with a selection of some data recently acquired at the summit (named Pizzo station, PZZ), to better understand the dynamic response of the two measurements sites to changes in environmental parameters during steady-state mild Strombolian activity.

Following the previously cited surveys, automatic radon monitoring started on September 2005 at selected sites, and after the eruptive crisis of February-April 2007, a real-time station was first installed at 520 m a.s.l. on the northeastern side of the cone (Fig.1). In October of the same year we deployed a second real-time station at the summit of the volcano (PZZ, located at 900 m a.s.l.). The first station is positioned between the N40°E and N60°E fracture zones (the main structural alignments of the island) at an approximate distance of 200 m. The site is on top of a 10-15 m deposit consisting of fine to coarse ash that lays above the Cannestrà lava flow. Conversely, the summit station PZZ is right above the N40°E fracture zone parallel to craters alignment, at a distance of about 150 m from the active fumaroles. Both stations are currently operative together with an automatic station located at the base of the cone (Punta Labronzo) where the data can periodically downloaded by means of a portable PC.

First, the time series for the data collected at the LSC station are reported in Fig. 6. Higher radon emissions approach 7200 Bq/m^3, whereas their average is 1700 Bq/m^3 (±1080) (see Table 2). It can be observed that the relative maximum in the activity of radon is reached in November 2007, with emissions of about 7200 Bq/m^3. The increasing trend is in good agreement with the one recorded by Carapezza et al. (2008) for CO_2 fluxes (up to ~ 4000 g / m^2 day) during the same span of time, characterized a sustained Strombolian activity (frequent explosions). A summary of the correlation coefficients between radon activities and environmental parameters is reported in Table 2 for both the real-time stations. Noticeably, the activity of radon is higher during the fall and winter and it substantially decreases during late spring and summer (with relative minima recorded during July-August 2007). Thus, there is an overall inverse correlation between the seasonal temperature variations and radon emissions. This phenomenon has been first noticed by Mogro-Campero and Fleischer (1977) who ascribed it to the summer time heating of the earth's surface: a seasonal inversion in the near surface temperature gradient affects the flow geometry of the convective cells, by creating a barrier to the upward migration of radon. Similar evidences have been found during high resolution radon monitoring at Somma-Vesuvius (Cigolini et al., 2001).

FIG. 6 TAB. 2 TAB. 3

At this station, the relationships between radon and atmospheric pressure time-series are more complex. Daily mobile averages seem to be somehow inversely correlated, but single minor peaks show that there are many exceptions. However, temperature is the parameter that seem to better rule radon emissions at the LSC station. Other interesting features are the cyclic peaks in radon (Fig. 6). In order to better understand the frequencies of these events, following the indications of Pinault and Baubron (1996), we performed signal processing analyses (Power Spectral Density, PSD) over the whole time series. In our case, by means of applying the Fourier transform we obtained the indicative frequencies reported in Fig. 7. It can be noticed that the radon signal includes major frequencies that match the combined effects of daily earth tides and temperature variations (every 12 hours), as well as the alternation of moon phases (~14.5 days and its multiple 29 days) together with moon-quarters (~7 days). Therefore, tidal forces seem to actively modulate radon degassing at Stromboli volcano supporting the general inferences of Barnet et al. (1997) on the occurrence of this process. Since radon is transferred to the surface by carrier gases (water and CO_2), these phases should be affected by such forces as well. The interplay between earth tides and Stromboli explosivity has been first noticed by Johnston and Mauk (1972).

FIG. 7

The selected time series recorded at PZZ is reported at Fig. 8 (Table 2). In this period radon activities are rather variable, with an average of ~ 7600 (± 3300) Bq/m^3 and higher emissions reaching 15600 Bq/m^3 (Table 2). It can be observed that radon fluxes are somehow positively correlated with atmospheric pressure and negatively correlated with temperature (Table 3). In particular, the increasing and decreasing trends of both radon and atmospheric pressure show that ^{222}Rn variations are somehow delayed in respect to changes in pressure: a span of time is required for obtaining the response of the “degassing” system to changing conditions. Correlation between ^{222}Rn activity, atmospheric pressure and water contents has been first observed by Zimmer and Erzinger (2003) during continuous monitoring of high temperature fumaroles at Merapi Volcano, Java. However, we further emphasize that the PZZ station is positioned along a summit fracture zone trending NE-SW and is located at about 150 m from the active fumaroles. The occurrence of the above correlation shows that the so called atmospheric "stacking effect" is operative at Stromboli. This process has the potential of reducing the efficiency of the convective cells that rule fluid motion within the hydrothermal system. Thus, the effect of this mechanism (also observed prior the paroxysmal explosion of April 5, 2003; cf., Cigolini et al., 2005) it is further proved by the fact that variations in soil temperatures are essentially decoupled from radon activity and atmospheric pressure. Therefore, a decrease in the efficiency of fluid degassing would cause a "longer permanence" of the hot fluids within the porous medium, generating a temperature increase in the surrounding soil.

FIG. 8

Conclusions

Previous surveys and real-time radon monitoring indicate that monthly average ^{222}Rn emissions may fluctuate under dynamic conditions that reflect changes in the volcanic activity as well as seasonal temperature variations. Moreover, maps obtained by plotting radon activities onto topographic DEM images support the idea that diffuse degassing is operative and efficient at Stromboli volcano.

We emphasize that real-time radon monitoring has been successfully tested at Stromboli volcano. The use of continuous-automated measurements by alpha spectrometry can be used to detect radon activities related to both diffuse and concentrated degassing. Recorded time series confirm a negative correlation between radon emissions and seasonal temperature variations. Signal processing analysis show that radon emissions may be actively modulated by tidal forces. In addition, radon activities recorded at the summit station located along a fracture zone are positively correlated with changes in atmospheric pressure. This may be explained with the onset of the "atmospheric stack effect" that may lower the efficiency of hydrothermal convection contributing to fluid pressure build up within the magma column, thus increasing volcano explosivity. In particular, the onset of the latter phenomenon should be carefully analyzed since a correlation among seismic signals and meteorological parameters (that may affect the dynamic behaviour of the magmatic system) has been recently emphasized (e.g., *Patanè et al*., 2007).

In conclusion, tidal forces and atmospheric pressure modulate degassing at Stromboli. However, if the system is sufficiently pressurized, it is not excluded that they may play an active role, together with self-sealing of hydrothermal fractures, in the triggering of major explosions. Future work will be focussed in analyzing volcano dynamics by means of these innovative and affordable technique for radon monitoring.

Acknowledgments. This research has benefited from funding provided by the Italian Presidenza del Consiglio dei Ministri - Dipartimento della Protezione Civile (DPC). Scientific papers funded by DPC do not represent its official opinion and policies. We thank R. Colozza and C. Cardaci for logistic support at Stromboli. The Stromboli topographic DEM image has been kindly provided by M.A. Marsella.

Figure captions

Fig. 1. Radon monitoring stations at Stromboli and the two major summit faults. Stars identify sites for real-time measurements: LSC and PZZ. The diamond is the location of the automated Labronzo Station. Full dots are stations for periodic measurements using track-etch detectors and E-PERM® electretes. The inset shows the location of Stromboli and the major structural features of the Aeolian arc.

Fig. 2. Histograms of average monthly radon emissions at Stromboli volcano (measured by a-track-etches, LR115, with a mean error of 12%) with the indication of variations in volcanic activity. Note that prior and during the onset of both major eruptive cycles radon emissions drastically increase. Histograms represent the average radon activity for each class of stations subdivided as: lower stations (below 100 m a.s.l.), summit stations (around the crater area) and other stations (cf. Fig. 1). The sum of the three represent the total monthly emissions of ^{222}Rn monitored at Stromboli.

Fig. 3. Topographic DEM images of average radon emissions onto the NE sector of Stromboli during the last major eruptive cycles. Periods of most active degassing refer to January-March 2003 and February-March, 2007, respectively. Black symbols represent measurement sites. Radon measurements were performed with E-PERM® detectors (which have a mean error of ~7 % on single measurements; Kotrappa et al., 1993) and represent average radon emissions integrated during their time of exposure.

Fig. 4. Spectral distribution of the different isotopes of the radon progeny detected by DOSEman for the LSC station during a year long monitoring. The lower portion of the graph reports the daily counts for each isotope (subdivided into Region of Interest, ROIs) cumulated for the whole year.

Fig. 5. Positioning the real-time radon station at the summit of Stromboli (PZZ station). Inset shows the inside of the station (contained in the polycarbonate case) with the dosimeter and the electronic board. This case has been inserted in the PVC box at about 30 cm from the bottom soil (see text for details).

Fig. 6. Time series for radon activity (Bq/m^3), atmospheric pressure (mbar) and soil temperature (°C) recorded at the Liscione station. Thicker curves represent weekly average values. The sampling time is 15 minutes.

Fig. 7. Normalized Power Spectral Density (PSD) for the whole year time series recorded at the LSC station. By utilizing the Fourier transform we obtained the above frequencies representative of periods that match the effects of daily earth tides and temperature variations, as well as the alternation of moon phases. The values for Ephemerids have been computed by transforming the sinusoidal signal composed by declination, distance and moon phases (original data for Stromboli coordinates were provided by INAF Catania).

Fig. 8. Selected recent time series for radon activity (Bq/m^3), atmospheric pressure (mbar) and ground temperature (°C) recorded at the summit Pizzo station (PZZ, from May 7, 2008 to June 5, 2008). Thicker curves represent daily average values.

References

Allard, P., Carbonnelle, J. , Metrich, N. , Loyer, H., Zettwoog P., 1994. Sulfur output and magma degassing budget of Stromboli volcano. Nature 368: 326-330.

Alparone, S., Behncke, B. , Giammanco, S., Neri, M., Privitera, E., 2005. Paroxysmal summit activity at Mt. Etna (Italy) monitored through continuous soil radon measurement. Geoph. Res. Lett. 2: L16307, doi:10.1029/2005GL023352.

Barberi, F., Innocenti, F., Ferrara, G., Keller, J., Villari, L., 1974. Evolution of Aeolian Arc volcanism (Southern Tyrrhenian Sea). Earth. Planet. Sci. Lett. 21: 269 – 276.

Barberi, F., Rosi, M., Sodi, A., 1993. Volcanic hazard assessment at Stromboli based on review of historical data. Acta Vulcanol. 3: 173-187.

Barberi, F., Civetta, L., Rosi, M., Scandone, R. 2008. Chronology of the 2007 eruption of Stromboli and the activity of the Scientific Synthesis Group. J. Volcanol. Geotherm. Res.

Beccaluva, L., Gabbianelli, G., Lucchini, F., Rossi, P.L., Savelli, C., 1985. Petrology and K/Ar ages of volcanic dredged from the Eolian seamounts: Implications for geodynamic evolution of the Southern Tyhrrenian basin. Earth Planet. Sci. Lett. 74: 187 – 208.

Bonaccorso, A., Calvari, S., Garfi, G., Lodato, L., Patanè, D., 2003. Dynamics of the December 2002 flank failure and tsunami at Stromboli volcano inferred by volcanological and geophysical observations. Geoph. Res. Lett. 30 (23): 2214, doi:10.1029/2003GL0188961941

Barnet, I., Prochazka, J., Skalsky, L., 1997. Do the earth tides have an influence on short-term variations in radon concentration? Rad. Prot. Dosimetry 69: 51-60.

Bonetti, R., Capra, L. , Chiesa, C. , Guglielmetti, A., Migliorini, C., 1991. Energy response of LR115 cellulose nitrate to α-particle beams. Nucl. Rad. Measur. 18: 321-338.

Calvari, S., Spampinato, L., Lodato., S., Harris, A.J., Patrick, M.R., Dehn, J., Burton, M., Andronico, D., 2005. Chronology and complex volcanic processes during the 2002-2003 flank eruption at Stromboli volcano (Italy) reconstructed from direct observations and surveys with a handheld thermal camera. J. Geophys. Res. 110: B02201, doi:10.1029/2004JB003129.

Carapezza, M.L., Inguaggiato, S., Brusca, L., Longo, M., 2004. Geochemical precursors of Stromboli 2002–2003 eruptive events. Geophys. Res. Lett. 31-7. doi:10.1029/2004GL019614.

Carapezza, M.L., Ricci, T., Ranaldi, M., Tarchini, L., 2008. Active degassing structures of Stromboli and variations in diffuse CO2 output related to the volcanic activity. J. Volcanol. Geoth. Res. (in press)Active degassing structures of Stromboli and variations in diffuse CO2 output related to the volcanic activity. J. Volcanol. Geotherm. Res. doi:10.1016/j.jvolgeores.2008.08.006.

Chiodini, G., Frondini, F., Raco, B., 1996. Diffuse emission of CO2 from the Fossa crater, Vulcano Island Italy . Bull. 2 Volcanol. 58, 41–50.

Chirkov, A.M. 1975. Radon as a possible criterion for predicting eruptions as observed at Karymsky volcano. Bull. Volcanol. 39: 126-131.

Cigolini C., Gervino, G., Bonetti, R., Conte, F., Laiolo, M., Coppola, D., Manzoni, A. , 2005. Tracking precursors and degassing by radon monitoring during major eruptions at Stromboli Volcano (Aeolian Islands, Italy), Geophys. Res. Lett. 32: L12308, doi:10.1029/2005GL022606.

Cigolini, C., Laiolo, M., Coppola, D., 2007. Earthquake-volcano interactions detected from radon degassing at Stromboli (Italy). Earth Planet. Sci. Lett. 257: 511-525.

Cigolini, C., Salierno, G., Gervino, G., Bergese, P., Marino, C., Russo, M., Prati, P., Ariola, V., Bonetti, R., Begnini, S., 2001. High-resolution Radon Monitoring and Hydrodynamics at Mount Vesuvius. Geoph. Res. Lett. 28 (21): 4035-4039.

Connors, C., Hill, B., La Femina, P., Navarro, M., Conway, M., 1996. Soil Rn-222 pulse during the initial phase of the June August 1995 eruption of Cerro Negro, Nicaragua. J. Volcanol. Geothermal Res. 73: 119-127.

Finizola, A., Sortino, F., Lenat, J.F., Valenza, M., 2002. Fluid circulation at Stromboli volcano (Aeolian Islands, Italy) from self-potential and CO2 surveys. J. Volcanol. Geoth. Res. 116: 1-18.

Fleischer, R. L., Mogro-Campero, A., 1985. Association with subsurface radon changes in Alaska and the Northeastern United States with earthquakes. Geochim. Cosmochim. Acta, 49: 1061-1071.

Giammanco, S., Sims, K.W., Neri, M., 2007. Measurements of 220Rn and 222Rn and CO2 emissions in soil and fumarole gases on Mt. Etna Volcano (Italy): implications for gas transport and shallow ground fracture. Geochem. Geophys. Geosyst. 8: Q10001 doi:10.1029/2007GC001644

Gründel, M., Postendörfer. J., 2003. Characterization of an electronic Radon gas personal Dosimeter. Radiation Protection Dosimetry 107 No. 4: 287–292.

Gillot, P.Y., Keller, J., 1993. Radiochronogical dating of Stromboli. Acta Vulcanol. 3: 69-77.

Heiligmann, M., Stix, J., Williams-Jones, G., Lollar, B.S., Garzon, G. V., 1997. Distal degassing of radon and carbon dioxide on Galeras volcano. J. Volcanol. Geotherm. Res. 77: 267-283.

Hernandez, P., Perez, N., Salazar, J., Reimer, M., Notsu, K., Wakita, H. 2004. Radon and helium in soil gases at Cañadas caldera, Tenerife, Canary Islands, Spain. J. Volcanol. Geotherm. Res. 131: 59-76.

Igarashi, G., Saeki, S., Takahata, N., Sumikawa, K., Tasaka, S., Sasaki, Y., Takahashi, M., Sano, Y., 1995. Ground-water Radon Anomaly before the Kobe Earthquake in Japan. Science 269: 60-61.

Johnston, M.J., Mauk, F.J., 1972. Earth tides and the triggering of eruptions from Mount Stromboli. Nature, 379: 708-711.

Kotrappa, P., Dempsey, J.C., Stieff, L.R., 1993. Recent advances in electret ion chamber technology. Rad. Prot. Dosim. 47: 461-464.

Mogro-Campero, A., Fleischer, R. L., 1997. Subterrestrial fluid convection: a hypothesis for long distance migration of radon within the earth. Earth Planet. Sci. Lett. 34: 321-325.

Neri, M., Lanzafame, G., 2008. Structural features of the 2007 Stromboli eruption. J. Volcanol. Geoth. Res. : doi:10.1016/j.jvolgeores.2008.07.021.

Patanè, D., Mattia, M., Di Grazia, G., Cannavo, F., Giampiccolo, E., Musumeci, C., Montalto, P., Boschi, E., 2007. Insights into the dynamic processes of the 2007 Stromboli eruption and possible meteorological influences on the magmatic system. Geophys. Res. Lett. 34: L22309, doi:10.1029/2007GL031730.

Pinault, J.L., Baubron, J.C., 1996. Signal processing of soil gas radon, atmospheric pressure and soil temperature data: a new approach for radon concentration modeling. J. Geophys. Res. 101: 3157-3171.

Planicić, J., Radolić, V., Vuković, B., 2004. Radon as an earthquake precursor. Nucl. Instr. Meth. in Phys. Res. S. A 530: 568-574.

Ripepe, M., Marchetti, E., Ulivieri, G., Harris, A.J., Dehn, J., Burton, M., Caltabiano, T., Salerno, G., 2005. Effusive to explosive transition during the 2003 eruption of Stromboli volcano. Geology 33/5: 341-344.

Rizzo, A., Grassa, F., Inguaggiato, S., Liotta, M., Longo, M., Madonia, P., Brusca, L., Capasso, G., Moricia, S., Rouwet, D., Vita, F., 2008. Geochemical evaluation of observed changes in volcanic activity during the 2007 eruption at Stromboli (Italy). J. Volcanol. Geotherm. Res. doi:10.1016/j.jvolgeores.2008.08.004.

Rosi, M., Bertagnini, A., Landi, P., 2000. Onset of persisting activity at Stromboli Volcano (Italy). Bull. Volcanol. 62: 294-300.

Sinclair, A.J., 1974. Selection of thresholds in geochemical data using probability graphs. J. Geochem. Explor. 3: 1929-149.

Streil, T., Oeser, V., Feige, S., 2002. An electronic radon dosimeter as a multipurpose device-a bridge between dosimetry and monitoring. Geofisica Internacional 41: 285-288.

Tinti, S., Maramai, A., Armigliato, A., Graziani, L., Manucci, A., Pagnoni, G., Zaniboni, F., 2006. Observations of physical effects from tsunamis of December 30, 2002 at Stromboli volcano, southern Italy. Bull. Volcanol., 68, 450-461.

Tibaldi, A., 2001. Multiple sector collapses at Stromboli volcano, Italy: How they work. Bull. Volcanol. 63: 112-125.

Varley, N.R., Armienta, M.A., 2001. The absence of diffuse degassing at Popocatepetl volcano, Mexico. Chem. Geol. 177: 157-173.

Williams-Jones, G., Stix, J., Heiligmann, M., Charland, A., Sherwood Lollar, B., Arner, N., Garzón, G.V., Barquero, J., Fernandez, E., 2000. A model of diffuse degassing at three subduction-related volcanoes. Bull. Volcanol. 62: 130-142.

Zimmer, M., Erzinger, J., 2003. Continuous H2O, CO2, 222Rn and temperature measurements on Merapi Volcano,Indonesia, J. Volcanol. Geoth. Res. 125: 25-38.

Fig. 1

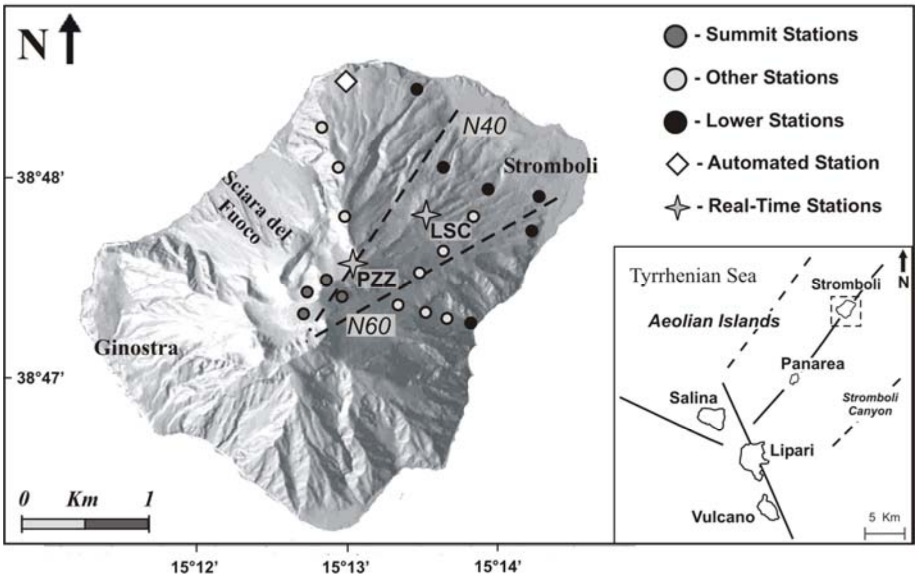
N
- Summit Stations
- Other Stations
- Lower Stations
- Automated Station
- Real-Time Stations
N40
Stromboli
38°48'
Sciara del Fuoco
LSC
PZZ
N60
Ginostra
38°47'
0 Km 1
15°12'
15°13'
15°14'
Tyrrhenian Sea
Stromboli
N
Aeolian Islands
Panarea
Salina
Stromboli Canyon
Lipari
Vulcano
5 Km

Fig. 2

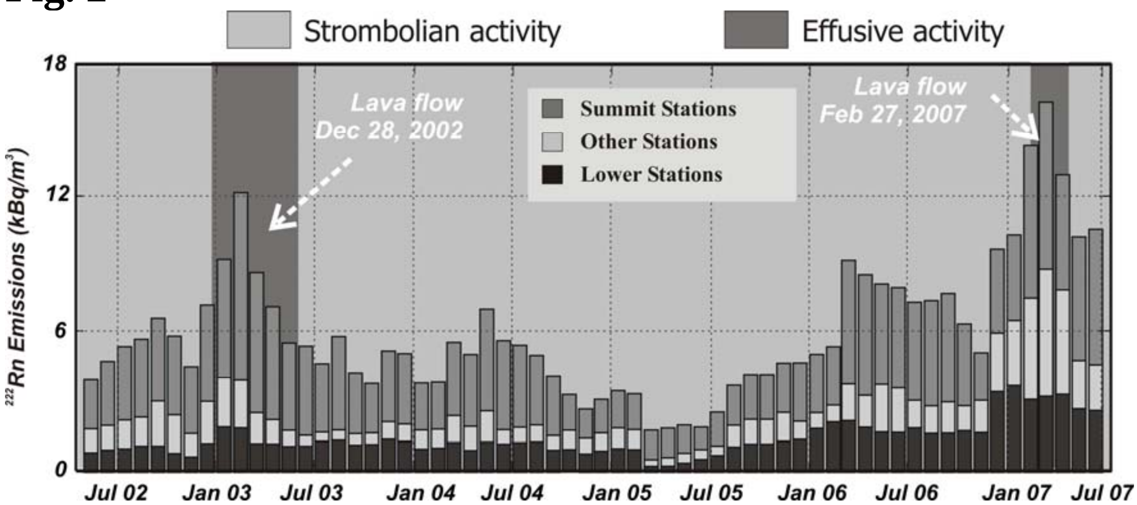
Strombolian activity
Effusive activity
Lava flow Dec 28, 2002
Summit Stations
Other Stations
Lower Stations
Lava flow Feb 27, 2007
222Rn Emissions (kBq/m3)
0
6
12
18
Jul 02
Jan 03
Jul 03
Jan 04
Jul 04
Jan 05
Jul 05
Jan 06
Jul 06
Jan 07
Jul 07

Fig. 3

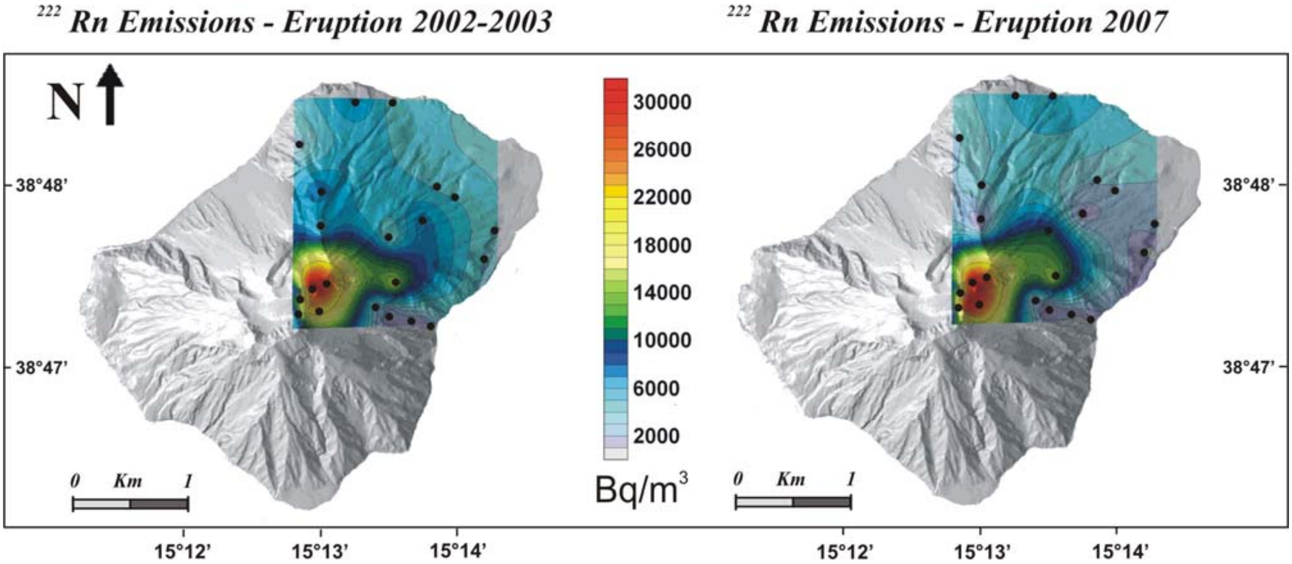
222 Rn Emissions - Eruption 2002-2003
222 Rn Emissions - Eruption 2007
N
38°48'
38°47'
30000
26000
22000
18000
14000
10000
6000
2000
Bq/m3
0 Km 1
0 Km 1
15°12'
15°13'
15°14'

Fig. 4

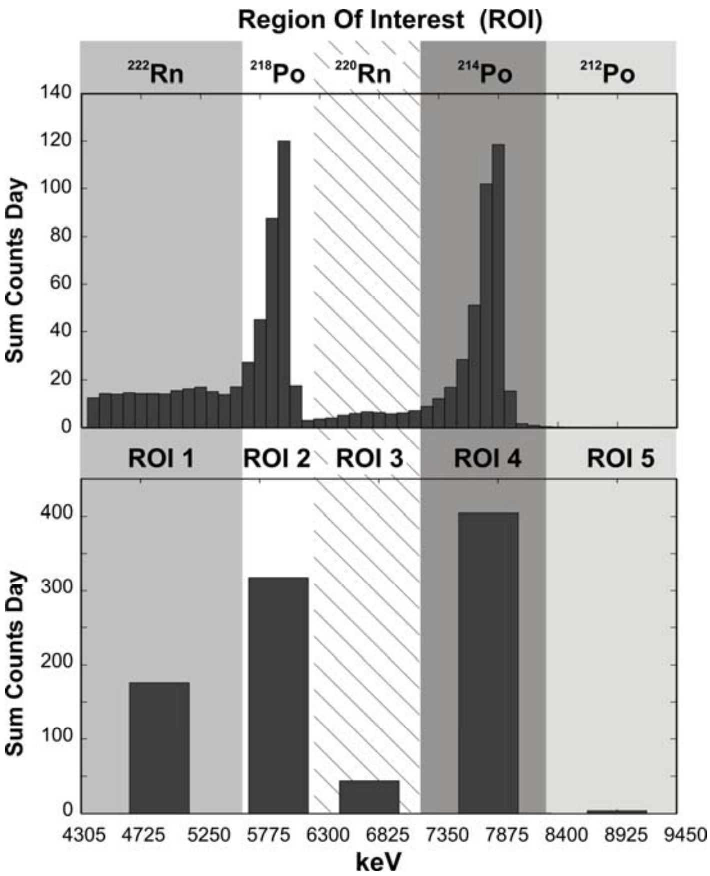
Region Of Interest (ROI)
222Rn
218Po
220Rn
214Po
212Po
Sum Counts Day
140
120
100
80
60
40
20
0
ROI 1
ROI 2
ROI 3
ROI 4
ROI 5
400
300
200
100
0
4305
4725
5250
5775
6300
6825
7350
7875
8400
8925
9450
keV

Fig. 5

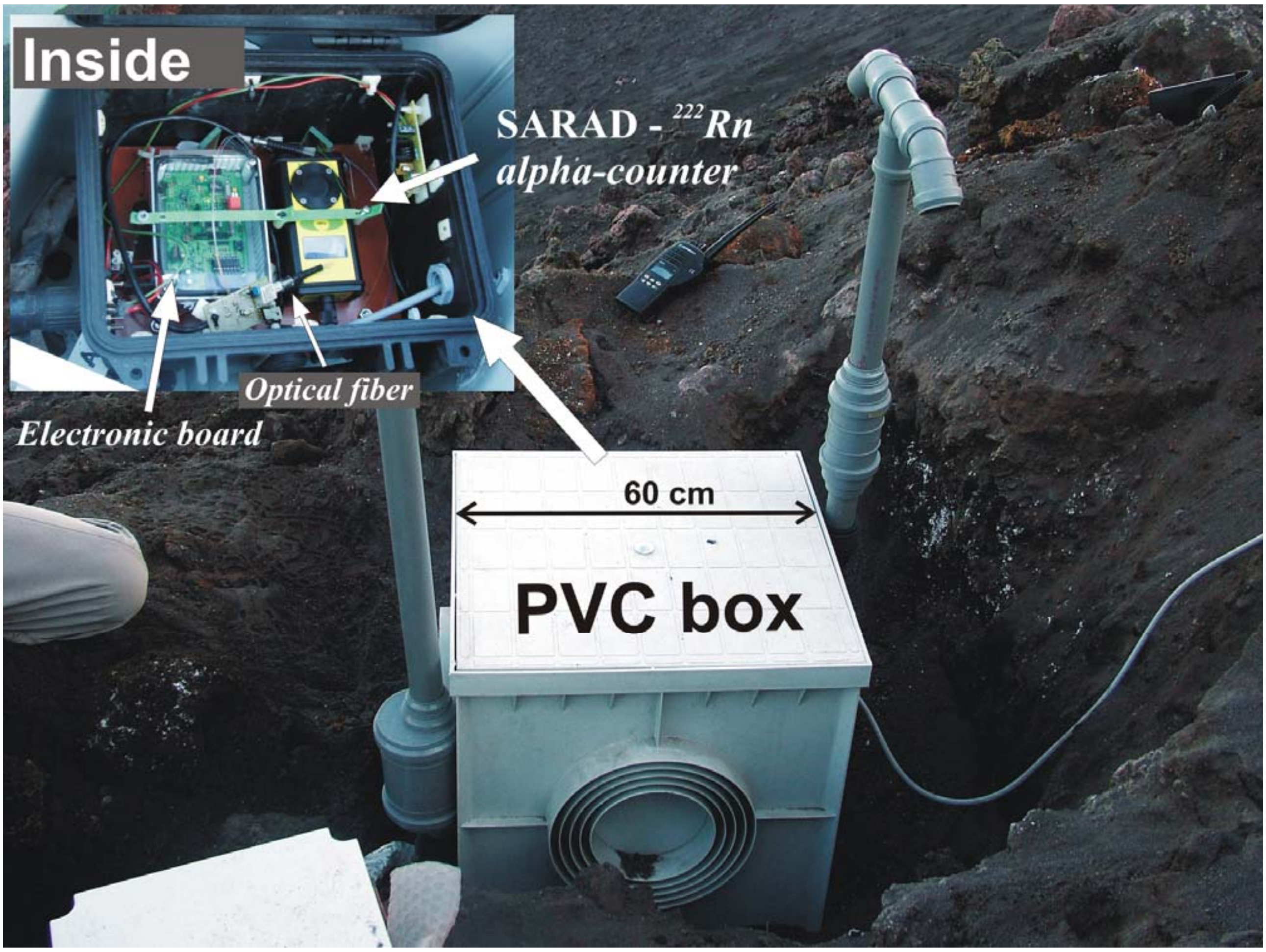

Inside
SARAD - 222Rn
alpha-counter
Optical fiber
Electronic board
60 cm
PVC box

Fig. 6

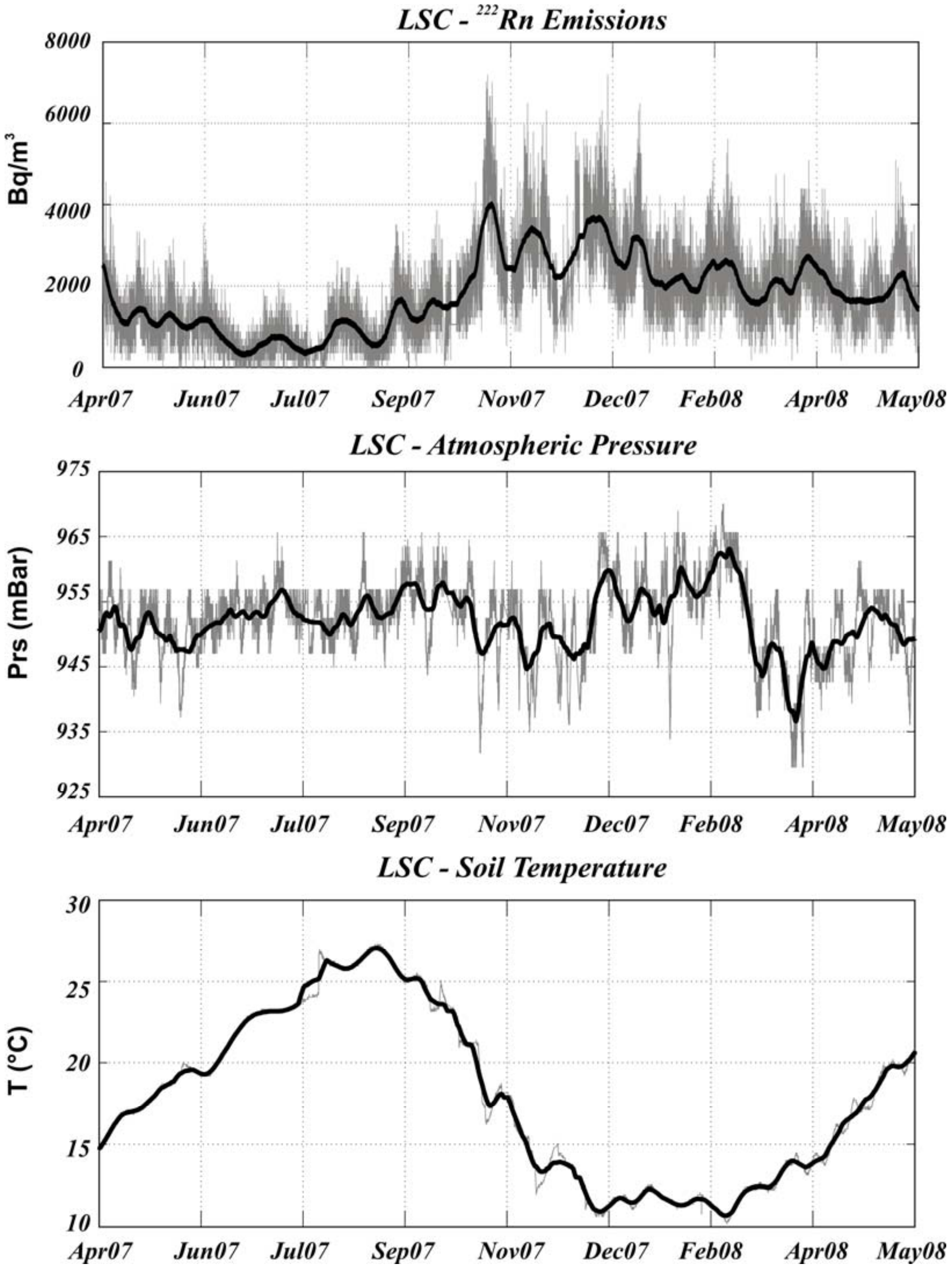
LSC - ^{222}Rn Emissions
Bq/m^3
8000
6000
4000
2000
0
Apr07
Jun07
Jul07
Sep07
Nov07
Dec07
Feb08
Apr08
May08
LSC - Atmospheric Pressure
Prs (mBar)
975
965
955
945
935
925
Apr07
Jun07
Jul07
Sep07
Nov07
Dec07
Feb08
Apr08
May08
LSC - Soil Temperature
T (°C)
30
25
20
15
10
Apr07
Jun07
Jul07
Sep07
Nov07
Dec07
Feb08
Apr08
May08

Fig. 7

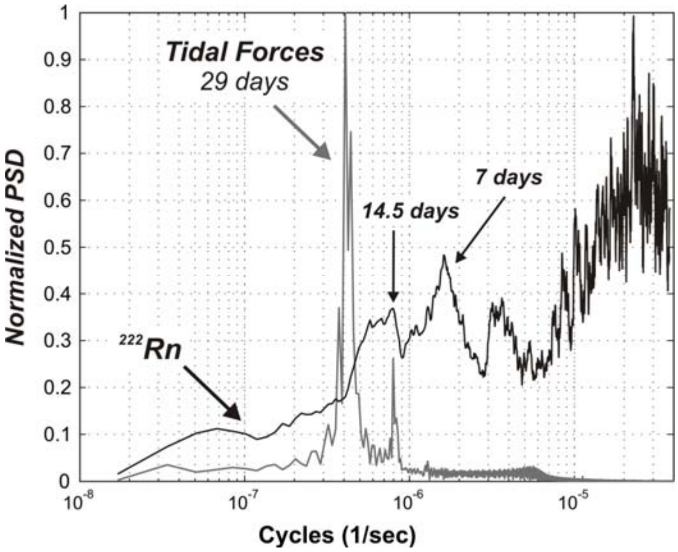

Tidal Forces
29 days
14.5 days
7 days
222Rn
Normalized PSD
Cycles (1/sec)

Fig. 8

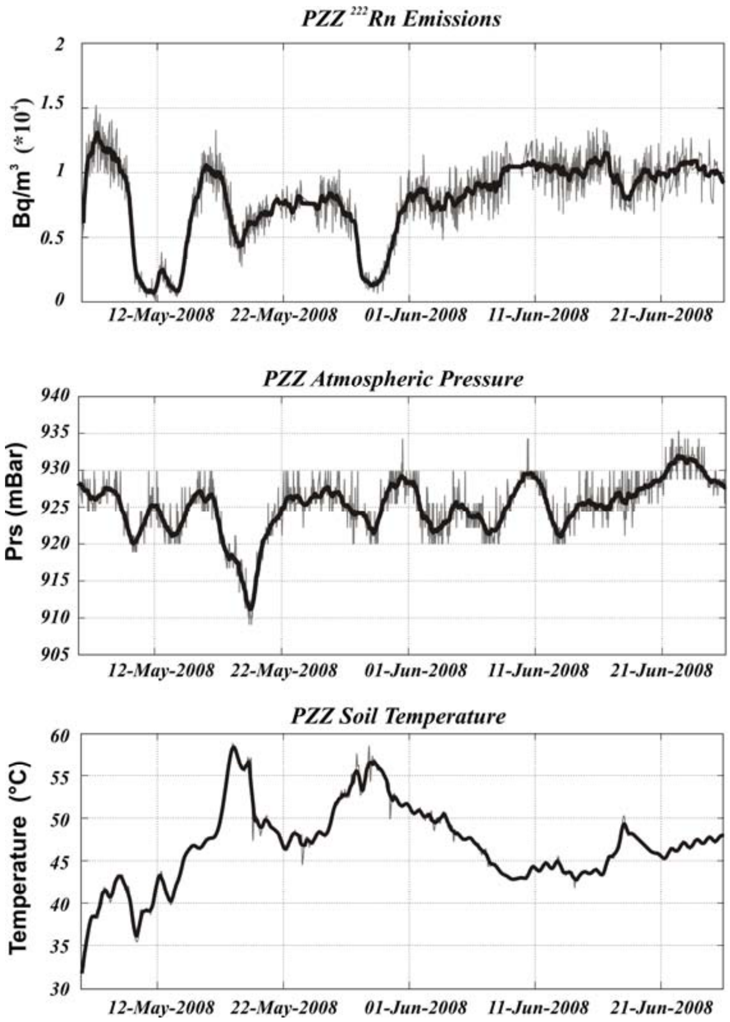

PZZ 222Rn Emissions
Bq/m3 (*10^4)
PZZ Atmospheric Pressure
Prs (mBar)
PZZ Soil Temperature
Temperature (°C)
12-May-2008
22-May-2008
01-Jun-2008
11-Jun-2008
21-Jun-2008

Table 1

Statistical analysis on the ^{222}Rn concentration by using E-PERM measurements from May 2002 to Sept 2007. Values are expressed in Bq/m^3 and have been obtained for earch station of the network, then the average for each group has been determined. A total of about 2300 measurements were collected within 5 years.

Location [a]	*background*	SD [b] (%)	*threshold*	SD [b] (%)	*anomalies*	SD [b] (%)
Lower stations	2114	37.03	5432	15.86	18907	60.47
Other stations	2435	54.99	6591	15.70	16840	33.69
Summit stations	6396	52.74	18430	16.20	41842	38.72

a Lower stations (below 100 m a.s.l.), Summit stations (around the crater area) and other stations are at intermediate altitude (between the two)

b SD: standard deviation

Table 2

Summary of the ^{222}Rn values acquired by the real-time stations currently operating at Stromboli

Stations	***LSC***	***PZZ***
N Data	16570	6820
Mean ($Bq\ m^{-3}$)	1770	8340
SD [a] ($Bq\ m^{-3}$)	1089	3050
Maximum ($Bq\ m^{-3}$)	7190	15614

a SD: standard deviation

Table 3

Correlations between ^{222}Rn activity and environmental parameters acquired by the real-time stations currently operating at Stromboli

	^{222}Rn ($Bq\ m^{-3}$)	Air P (mBar)	Soil T (°C)
LSC station			
^{222}Rn ($Bq\ m^{-3}$)	1	-0.07	-0.55
Air P (mBar)	-0.07	1	0.04
Soil T (°C)	-0.55	0.04	1
PZZ station			
^{222}Rn ($Bq\ m^{-3}$)	1	0.26	-0.59
Air P (mBar)	0.26	1	-0.34
Soil T (°C)	-0.59	-0.34	1